PERFORMANCE ASSESSMENT OF PARABOLIC TROUGH SOLAR COLLECTORS

A DISSERTATION

SUBMITTED IN PARTIAL FULFILLMENT OF THE REQUIREMENTS FOR THE AWARD OF THE DEGREE OF

MASTER OF TECHNOLOGY

IN

THERMAL ENGINEERING

Submitted by:

Anshul Tewari

(2K18/THE/01)

Under the supervision of

PROF. R.S. MISHRA

DEPARTMENT OF MECHANICAL ENGINEERING

DELHI TECHNOLOGICAL UNIVERSITY

(Formerly Delhi College of Engineering)

Bawana Road, Delhi-110042

AUGUST, 2020

DEPARTMENT OF MECHANICAL ENGINEERING

DELHI TECHNOLOGICAL UNIVERSITY

(Formerly Delhi College of Engineering)

Bawana Road, Delhi-110042

CANDIDATE'S DECLARATION

I, **Anshul Tewari**, Roll No. **2K18/THE/01** student of M.Tech (Thermal Engineering), hereby declare that the project Dissertation titled "**Performance Assessment of Parabolic Trough Solar Collectors**" which is submitted by me to the Department of Mechanical Engineering, Delhi Technological University, Delhi in partial fulfillment of the requirement for the award of the degree of Master of Technology, is original and not copied from any source without proper citation. This work has not previously formed the basis for the award of any Degree, Diploma Associateship, Fellowship or other similar title or recognition.

Place: Delhi

Date: 26 August 2020

ANSHUL TEWARI

(2K18/THE/01)

DEPARTMENT OF MECHANICAL ENGINEERING

DELHI TECHNOLOGICAL UNIVERSITY

(Formerly Delhi College of Engineering)

Bawana Road, Delhi-110042

CERTIFICATE

I hereby certify that the Project Dissertation titled "**Performance Assessment of Parabolic Trough Solar Collectors**" which is submitted by **Anshul Tewari**, Roll No. **2K18/THE/01** Department of Mechanical Engineering, Delhi Technological University, Delhi in partial fulfillment of the requirement for the award of the degree of Master of Technology, is a record of the project work carried out by the student under my supervision. To the best of my knowledge this work is original and carried by the student himself.

Place: Delhi

Date: 26 August 2020

PROF. R.S. MISHRA

SUPERVISOR

Department of Mechanical Engineering

Delhi Technological University, Delhi

ACKNOWLEDGEMENT

I take this opportunity to express my profound gratitude and deep regards to my guide **Prof. R.S. Mishra**, Department of Mechanical Engineering, Delhi Technological University, Delhi for his exemplary guidance, monitoring and constant encouragement throughout the course of this project report. The blessings, help and guidance given by him time to time shall carry me a long way in the journey of life on which I am about to embark.

I also take this opportunity to express a deep sense of gratitude to the faculties of Department of Mechanical Engineering, Delhi Technological University, Delhi for their cordial support, valuable information and guidance, which helped me in completing this task through various stages.

ANSHUL TEWARI

M.TECH (THERMAL ENGINEERING)

2K18/THE/01

ABSTRACT

In this study, a detailed parametric study of a solar parabolic trough collector is presented. The current condition of our environment compels us to restrain our use of fossil resources for energy production. It is our immediate priority to shift to renewable sources of energy which are non polluting and can be replenished in a short amount of time. Solar energy is a feasible option before us to fulfill our energy requirements. Concentrating solar collectors make use of the solar irradiation falling over the surface of the Earth. The high concentration ratios of collectors have the potential to transform the solar insolation into high heat energy. This energy may be used for a number of purposes like power production, process heating, refrigeration and many more. Parabolic trough solar collectors are widely used all over the globe as they can produce temperatures as high as 300°C. They are a type of line focusing solar collectors equipped with sun tracking mechanism. In this project, a mathematical model is formulated in EES of a parabolic trough solar collector and various parameters of it are calculated from the input conditions. The parameters like temperature of receiver, collector heat removal factor, overall loss coefficient, thermal efficiency of collector and optical efficiency are calculated and plotted in the form of a curve. This parametric calculation is carried out for every month of the year at different time intervals and all the values are tabulated and presented in the form of a curve. It is inferred from the calculations that the maximum thermal efficiency is obtained for the month of May which is 59.57%. Also, the properties are modeled at different mass flow rate of thermic fluid at different time of the day to get a fair idea about how the output characteristics vary with the variation in input

parameters. Three values of mass flow rate are used in this study that are 0.0986 kg/s, 0.0886 kg/s and 0.0786 kg/s and the corresponding variation in properties is presented in the form of a curve. It is also observed that the efficiency of the collector increases if the flow rate of heat transfer fluid is increased. However, the fluid exit temperature increases with the decrease in mass flow rate of heat transfer fluid.

TABLE OF CONTENTS

Candidate's Declaration **i**

Certificate **ii**

Acknowledgement **iii**

Abstract **iv**

Table of Contents **vi**

List of Figures **viii**

List of Tables **x**

Nomenclature **xi**

CHAPTER 1 INTRODUCTION **1-7**

1.1 Renewable Energy in India 2

1.2 Solar Energy in India 4

1.3 Concentrating Collectors 4

1.3.1 Parabolic Trough Collectors (PTC) 6

CHAPTER 2 LITERATURE REVIEW **8-13**

2.1 Conclusions from Literature Review 12

2.2 Research Gap 13

2.3 Objective 13

CHAPTER 3 SYSTEM DESCRIPTION 14-16

CHAPTER 4 MATHEMATICAL MODELING 17-19

CHAPTER 5 RESULTS AND DISCUSSION 20-32

5.1 Results of Year-Round Performance Examination 23

5.2 Results of Fluid Flow Rate Variations 28

CHAPTER 6 CONCLUSIONS AND FUTURE SCOPE 33-34

6.1 Conclusions 33

6.2 Future Scope 34

References 35

Appendix 1 38

Appendix 2 40

Appendix 3 44

LIST OF FIGURES

CHAPTER 1 INTRODUCTION

Fig. 1.1 Installed capacity in MW by source on December, 2019 2

Fig. 1.2 Cumulative achievement in renewable energy (MW) by December, 2019 3

Fig. 1.3 Parabolic trough collector with its parts 7

CHAPTER 3 MODELING METHODOLOGY

Fig. 3.1 Cross section of solar PTC with nomenclature 15

CHAPTER 5 RESULTS AND DISCUSSION

Fig. 5.1 Year round variation in beam radiation with time 24

Fig. 5.2 Year round variation in thermal efficiency with time 25

Fig. 5.3 Year round variation in rate of useful heat gain with time 26

Fig. 5.4 Year round variation in overall loss coefficient with time 26

Fig. 5.5 Year round variation in heat removal factor with time 27

Fig. 5.6 Year round variation in fluid exit temperature with time 28

Fig. 5.7 Variation in useful heat gain with time for different flow rates 29

Fig. 5.8 Variation in Overall loss coefficient with time for different flow rates 30

Fig. 5.9	Variation in heat removal factor with time for different flow rates	30
Fig. 5.10	Variation in thermal efficiency with time for different flow rates	31
Fig. 5.11	Variation in exit temperature of fluid with time for different Flow rates	32

LIST OF TABLES

CHAPTER 3 MODELING METHODOLOGY

Table 3.1 Characteristics of the system 16

CHAPTER 5 RESULTS AND DISCUSSION

Table 5.1 Validation of current model with the results in [12] 20

Table 5.2 Input parameters used for validation of model with [9] 21

Table 5.3 Validation of the model against results in [9] 21

Table 5.4 Input parameters used for validation of model with [19] 22

Table 5.5 Validation of the model against results in [19] 23

NOMENCLATURE

D	Diameter
W	Aperture of Concentrator
L	Length of Concentrator
x	Tape twist ratio
T	Temperature
C	Concentration ratio
P	Pressure
I_b	Hourly beam radiation
r_b	Tilt factor
Q_u	Useful heat gain rate
S	Absorbed flux
U_l	Overall loss coefficient
F_r	Heat removal factor
Cp	Specific heat
$\dot{m}$	Mass flow rate
F’	Collector efficiency factor
h	Heat transfer coefficient
N_u	Nusselt number
P_r	Prandtl number
Re	Reynold number

Greek letters

ρ	Reflectivity of concentrator
τ	Transmissivity of glass cover
γ	Intercept factor
ε_c	Emissivity/absorptivity of glass cover
ε_p	Emissivity/absorptivity of absorber tube
ηi	Instantaneous efficiency of collector
ηo	Optical efficiency of collector
ω	Hour Angle

Subscripts

fo	Fluid exit
fi	Fluid inlet
pm	Mean plate
c	Cover
o	Outside
i	Inside
f	Fluid
a	Ambient

CHAPTER 1

INTRODUCTION

Energy is the fundamental requirement for human civilization to function. For centuries we have relied on fossil sources of energy to satisfy our demand, but these sources are limited and also cause environmental pollution and are primarily responsible for the degradation that has been caused in our environment. In order to limit the increase in pollution levels and deal with the energy demand simultaneously, we must look up for resources of energy that are capable to meet our requirements and can also limit the environment degradation. Renewable energy is the way forward in achieving this feat. Renewable sources of energy are non polluting, can be replenished in a shorter period of time as compared to the fossil resources and are equally capable to supply us the required energy for our development. Every nation across the world is stretching their potentials to unravel new technologies that can supply the required energy with better efficiencies of conversion. Various global agencies and organizations have been made to check the deterioration of environmental resources caused by the combustion of polluting sources of energy like fossil fuels. Global summits are also planned periodically that emphasize on development of new technologies and make technology development feasible for developing countries as well through technology transfer by developed and technologically ahead nations. Some conventions also focus on limiting the environmental pollution and ascertain the limits of pollution for every country.

The aforementioned discussion describes the immediate need to shift our energy scope towards the non polluting and easily replenished sources of energy as well as the measures that are taken to check that the awareness is widespread about the potential of non polluting energy. A variety of energy sources are available in the nature that can satisfy the global energy needed, they are solar energy, wind energy, tidal energy, geothermal energy and many more. A lot of effort is prevalent throughout the globe to enhance maximum energy from the naturally occurring energy sources. With the emergence of new, improved and advanced technology in

the field of renewable energy, the efficiencies of conversion have improved significantly and also the cost occurring in them will be reduced making them affordable for all sections of the society.

Fig. 1.1 shows the installed capacity in MW with respect to its source of production by December, 2019. It can be derived that the majority of energy is still supplied by thermal sources but it is evident that the share of non polluting sources is also increasing. The government is also taking essential steps to promote the use of these sources to satisfy the energy demands.

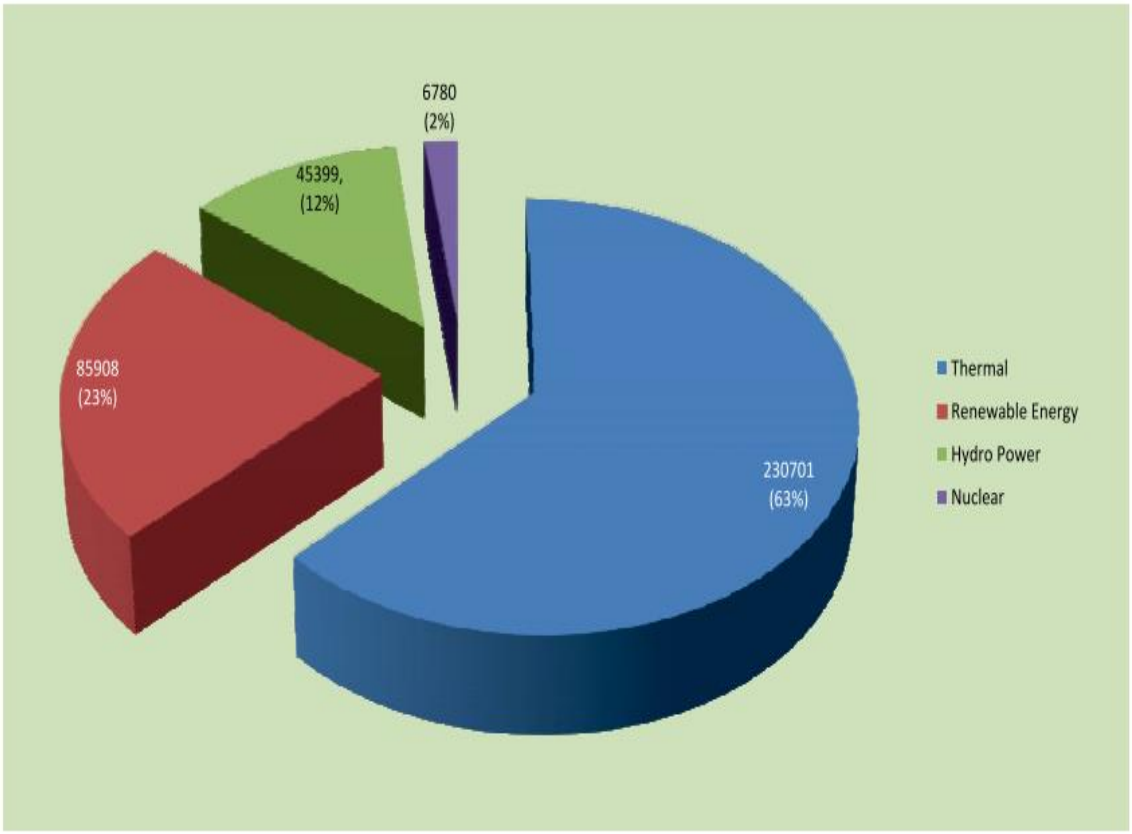

Fig. 1.1 Installed capacity in MW by source on December, 2019 [1]

1.1. Renewable Energy in India

India still produces a majority of its energy from fossil based sources but our country is determined to change this prospect in near future. A number of projects are underway currently in India that focus on unearthing the renewable potential of India. The technology sector is taking leaps in the energy sector to make the energy

from non polluting sources economically viable for everyone. Various governments in the country have focused on non polluting energy sources and efforts have been made to unleash the maximum potential of these sources for nation building with future sustainability in mind. Fig. 1.2 depicts the sector wise cumulative achievement made in the field of non polluting energy in MW by December of 2019. It can be seen that wind power among all the sources is developed most in our county and its supplies are the highest, followed by solar power.

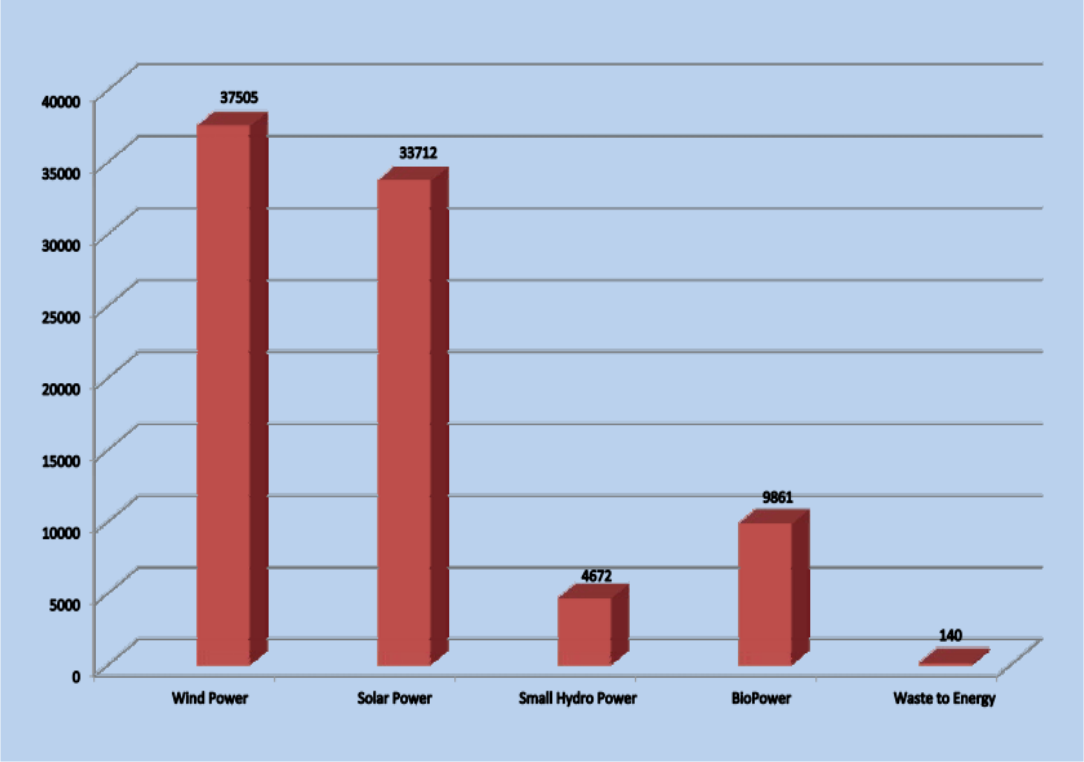

Fig.1.2. Cumulative achievement in renewable energy (MW) by December, 2019 [1]

India has set an aim to produce 175 GW of usable power from Renewable sources by 2022 and will increase the installed capacity of electricity from non fossil based resources to 40% [1]. Also, India will reduce its carbon emission by increasing the area under tree cover. With a population of 1.3 billion people, India is third amongst the countries with highest electricity consumption. The National Action Plan on Climate Change (NAPCC) was put in place to deal with the change in climate and the National Solar Mission was the first mission to operate under NAPCC in 2010. Under this mission, the solar power capacity is to be increased to 100 GW by 2022.

1.2. Solar Energy in India

The installed capacity of solar power in India is 33.73 GW as on December 2019 and the target for 2019-20 and 2020-21 is 30 GW each [1]. Karnataka is the state with highest solar installed capacity of 7274.92 MW, followed by Rajasthan with 4844.21 MW, Tamil Nadu with 3788.36 MW, Telangana with 3620.75 MW, Andhra Pradesh with 3559.02 MW. Delhi has a capacity of 156.12 MW [1]. Solar energy is intermittent in nature therefore, it is justified to use thermal storage in order to harness this energy even with absence of sunlight like at night. India is blessed with nearly 3,000 hours of sunshine every year. The solar radiation received on the Indian subcontinent is immense due to its geographical location near the equator. The ministry has sanctioned two pilot projects of 40 KW and 10 KW employing concentrated solar for power generation along with 24*7 thermal storage. Also, subsidies will be provided to access 75% of concentrated solar project cost. All these efforts are being made to make people aware about the benefits of renewable energy and together making it feasible for people from all the sections of the society to take advantage of these resources.

1.3. Concentrating Collectors

Concentrating collectors increase the power of solar radiation up to many times by focusing them on a smaller area, unlike flat collectors which simply reflect light without concentrating it. Flat plate collectors are deficient when the work involves high temperature applications. The highest temperature that can be obtained using a flat plate collector is far below the temperature range achievable with the use of concentrating collectors. Therefore, the usability of flat plate collectors is limited to low temperature employing applications only. To enhance their usage, some flat plate collectors are equipped with reflectors at their ends. These reflectors improve the concentration ratio for flat plate collectors from one to a higher value and thereby the highest temperature derived from this system also increases. But these setups still cannot match the high temperature employability of concentrating collectors and lag behind primarily because the concentration ratio that can be derived from

concentrating collectors are higher than those in flat plate collectors and flat plate collectors with reflector attachments.

Owing to this inherent property of concentrating collectors, they can produce much higher temperature range than the flat plate collectors. The global radiation received over the surface of the Earth is divided into two parts, direct beam radiation and diffuse radiation. Direct beam radiation is the part of solar radiation that reaches the concentrating collector without any hindrance. Diffuse radiation is that part of solar radiation that is diffused by the atmosphere, air molecules, clouds, aerosols, dust particles and vapors. This radiation when reaches the concentrator, it cannot be focused to the receiver and is of not much use for energy generation by the concentrating collector. For beam radiation to reach the concentrator, it is required that the concentrating collectors be installed in place with higher number of clear sky days to avoid loss in the form of diffuse radiation. To increase its performance, concentrators tend to reduce their incidence angle with the solar radiation to a minimum and use sun tracking for this purpose. The Sun tracking mechanisms follow the position of the Sun throughout the day and increase the availability of solar radiation.

There are mainly four types of concentrating collectors:

- Parabolic Trough Collectors (PTC)
- Solar Power Tower
- Linear Fresnel Reflector
- Parabolic Dish Collector

Solar tower is a type of point focusing concentrating collector in which the heliostats focus the solar insolation over the receiver. The receiver is placed over a tower and thermal fluid gets heated by the focused solar radiation. Linear Fresnel Reflector comprises of mirrors that reflect the incident radiation over a downward facing reflector that is present at the focal point of the mirrors. It is a line focusing concentrator. A Parabolic Dish Collector has a paraboloid geometry concentrator in the form of a dish. It is a point focus concentrator with the point of focus at the focal point of the concentrator dish.

Out of these types, PTC is the most developed and widely used concentrating collector because it can achieve much higher temperatures without much loss in collection efficiency [2].

1.3.1. Parabolic Trough Collectors (PTC)

A parabolic trough solar collector is amongst type of concentrating collectors that is equipped with a linear parabolic concentrator the focuses the solar irradiation onto a receiver that is positioned at the focal axis of the concentrator. It gets its name from the parabolic shape of its concentrator surface. PTC is a type of line focusing concentrating collector where the concentrated solar radiation transfers its energy to an absorber tube. It generally employs single axis sun tracing mechanism to reduce the angle of incidence between the concentrator and incident solar radiation. Temperature range of 150°C to 350°C is achievable in this system. The solar radiation received over the surface of the concentrator is focused on the receiver where the heat transfer fluid is present in the absorber tube. High concentration ratios of a PTC are capable of producing large amounts of heat energy in the absorber tube by the conversion of solar energy. This large heat energy is supplied to the heat transfer fluid circulating in the absorber tube. The enthalpy of the fluid increases after this heat transfer along with its capability to do work. This work may be used for a variety of purposes like power generation in a turbine or may be using the heat energy of the fluid in process heating or refrigeration.

Fig.1.3 depicts a parabolic trough collector with its basic functionality describing the working of the system. The parabolic concentrator is equipped with reflective surface that concentrates the rays of the sun over the receiver. The receiver, which is in the form of a tube, is shown with its inlet and outlet for thermic fluid. The receiver runs along the linear dimension of the parabolic concentrator. This tube also has a cover to decrease the radiation losses. The energy of the fluid is higher at outlet than the energy that was available with the fluid at the inlet.

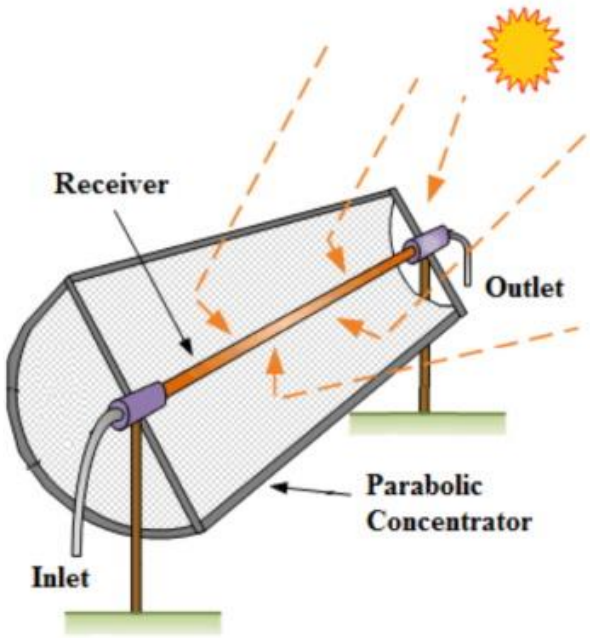

Fig.1.3. Parabolic trough collector with its parts [18]

CHAPTER 2

LITERATURE REVIEW

Huang et al. [3] proposed an analytical model and integration methodology for simulation of performance analysis of PTC incorporated with vacuum tube as receiver. This model, analytically derives the optical efficiency at each point of the reflector which is then used to simulate the optical efficiency of the system using numerical integration methodology. It also analyses the effects of various losses and errors on the system's efficiency.

Siva Subramanian et al. [4] tested a parabolic trough solar collector without sun tracking equipped with different material over the surface of the absorber. It stated that the output results vary by using different materials as the surface of the absorber. Aluminium sheet, Aluminium foil and mirror sticker were used as the surface of the absorber of parabolic trough collector to record the output parameters. It was concluded that the maximum efficiency of the parabolic trough solar collector is obtained when using aluminium sheet as the material of the absorber surface.

Quezada-Garcia et al. [5] developed a mathematical model of a parabolic trough solar collector with known profiles of axial and radial temperature to evaluate the steady state heat transfer. An iterative procedure in Python software was developed along with a visualisation system. This model employs water, nanofluids and thermal oil as heat transfer fluid and finds that the efficiency is higher in case of nanofluids having increased volume fraction of particles. Thermal efficiency is 80% for 0.04 volume fraction and 79% for 0.02 volume fraction of particles in nanofluid. However, the lowest efficiency of the system is 76% obtained with thermal oil. This study concludes that low pressure working conditions are allowed when using nanofluids as heat transfer fluid instead of pressurised water.

Arun and Sreekumar [6] worked on a water desalination setup that employs solar energy. This experimental study employs a parabolic trough collector equipped with sun tracking to focus the solar insolation over the the absorber through which saline

water is flowing. The water was converted into steam by absorbing this heat and the steam was further condensed at the observer outlet and drinkable water was formed. This study works with two materials of absorber tube which are stainless steel and a copper tube covered with glass. It was inferred that the copper tube with glass cover had better performance than the Stainless Steel Tube. The drinkable water was available at 2 litres per square metre with an efficiency of 12.74%. Finally, it was concluded that water desalination using PTC results in hardness and chemical levels below established limits.

Conrado et al. [7] stated detailed thermodynamic aspects of a parabolic trough collector that are vital for its future developments, by considering different mathematical modelling, numerical techniques, simulation and experimental methodology. It further presented an economic viewpoint for parabolic collectors. It concluded that the techniques applicable for this system to be feasible for the market and economic management in its designing fabrication and operation are vital for future development.

Qu et al. [8] found that commercial PTC setup had a poor efficiency of 50% which was due to the higher cosine losses. These losses decrease by decreasing the solar incidence angle which further changes with the collector surface azimuth angle. 300 kilowatt PTC collector was developed with rotatable axis. The cosine losses are minor in summers, so North South tracking is employed. However, these losses are significant in winters and in order to reduce the incidence angle of incoming solar insolation, the collector is rotated and the cosine losses are decreased along with increased solar insolation. This work concludes that the average reduction in cosine loss per day is 10.3% whereas the increase in efficiency is 5% with respect to north south tracking collector.

Kumar and Kumar [9] modeled a parabolic trough collector on the basis of temperature of the receiver wall. It used a coating of black paint and a glass cover on the receiver tube. The results obtained by using this model on a PTC were in accordance to the experimental results. It was inferred that the maximum increase in water temperature for horizontal plane was 11.1 degrees and that for an inclined plane was 12.2 degrees with a flow rate of 0.010 kgs per second. It was also able to

achieve peak thermal efficiency of 66.78% for horizontal plane and 65.7 7% for inclined plane.

Lozano-Medina et al. [10] presented design analysis for the configuration and installation of cylindrical parabolic solar collector to be installed in a hotel in the the Canary Islands of Spain. It presents a comparison between concentrated solar power, solar photovoltaic and plane solar collectors to be used for the purpose of energy production. It also considered the economic feasibility of the project to suit the requirements of the hotel. It concluded that the cost of energy using a PTC is competitive with that of PV technology and further developments would result in cost reduction.

Zou et al. [11] presented a special parabolic trough collector of small size to be used for water heating in colder areas. It found that in cold areas traditional flat plate collectors pose serious problems of heat loss reduce efficiency freezing and bursting of tubes. The efficiency was increased when the fluid temperature was below 100°C and would further increase with the fluid temperature. However, frosting and high wind velocities, especially in the morning significantly reduced the efficiency to below 26%. It concluded that at minor disturbances the efficiency was stable at 67%, depicting that the system beared anti freezing properties and is suited for the colder areas.

Zou et al. [13] described the effects of deviation of optical parameters from the ideal condition. These parameters include incident angle and optical errors. It was observed that the hindrance in distribution of heat flux is the most important cause of performance deterioration of PTC. Deviations in optical parameters cause losses in the collector which greatly influence its efficiency. It was observed that the reduction in efficiency by the variation in incidence angle is 41.11% . Moreover, the influence in the collectors performance by the various types of losses was also examined and it was concluded that the deviation in these parameters is responsible for both performance reduction and affecting the life of the absorber due to overheating.

Aguilar et al. [14] considered a model for heat transfer to assess performance of a PTC working on varying heat transfer fluids. It was expressed that the

transformation efficiency of solar radiation into electrical energy can be improved by using fluids at much higher temperature or by using supercritical heat transfer fluids. This model considered thermal oil or synthetic oil along with carbon dioxide, both in subcritical and supercritical state. The temperature of fluid at the exit and the efficiency of collectors are considered as the parameters to examine the performance of the collector. The results derived from this model are near in proximity with those derived using experimental results. Moreover, collector working with the supercritical state of carbon dioxide was subjected to varying input variables like flow rate, inlet temperature of fluid and varying radiation. It was concluded that the varying radiation had the most significant effect on output and operation of the PTC.

Khakrah et al. [15] carried out energy as well as exergy analysis on a PTC. Various parameters that are associated with this study were varied. Nanoparticles were used with the heat transfer fluid as additives and their impact on the collector performance was examined. The input variables considered to the system were varied and their influence on the system efficiency was derived. It was concluded through study that the behavior of thermal efficiency and that of exergy efficiency were opposite when the inlet temperature was varied. The increase in temperature of incoming fluid resulted reduced thermal efficiency but an increase in exergy efficiency. Similarly, the effect in both these efficiencies with deviations in the speed of the wind were expressed as being almost similar.

Bellos and Tzivanidis [16] focused on improving the design of PTC in order to increase its total effectiveness. The complete system was analyzed and the possible and essential modifications were expressed. The goal of the study was to modify the current technologies in PTC into improved developments that are compact and cost-effective by producing higher thermal efficiencies and higher fluid temperatures at the outlet . The modifications were introduced in several stages and their effect on the system was also described. The optical modifications deal with the optical properties of the system and work on the introduction of new technologies, like secondary reflectors, in order to achieve uniformity in the heat flux that is absorbed. Similarly, the modifications in the field of thermal science were the use of better heat transfer fluids with the help of additives like nanofluids and also, by devising improved receiver designs with better capabilities.

Tyagi et al. [17] studied the parametric performance as well as the exergy analysis of a PTC considering the solar radiation for an hourly basis. The goal was to increase the exergy performance and to improve the outputs derived from the system. Various input parameters were changed and an attempt was made to achieve a trade off between the inputs, in order to achieve the maximum output. For a given solar intensity, the effect on exergic efficiency by varying the concentration ratio was observed. It was stated that as the concentration ratio increases, owing to higher values of temperature, the losses by radiation are also higher. These high value of loss results in a decreased exergy performance. Similarly, the results were obtained by considering variation in solar insolation and it was summed up that the influence of flow rate is vital in collector's performance and thereby, be chosen cautiously.

2.1. Conclusions from Literature Review

The literature reviews presented in this study emphasize primarily on increasing the performance of the concentrator system. The various techniques employed for this purpose are also discussed along with their influence on properties. It can be stated that parabolic trough collector are vastly employed all over the world for a wide variety of applications. The desalination of water, water heating in colder areas are some fields of its application. Also, focus was set in order to increase the operating characteristics of the PTC system. Use of nanofluids and other heat transfer fluids is an attempt in the direction of improving the working of the system. A number of models and simulations are carried out in different computer tools in order to assess the role of performance improvement techniques on the system. The results presented were validated using experimental investigation in order to prevent any modelling errors. The optical errors arising out of the system were addressed and attention was paid to keep them to a minimum. The materials of construction of the reflector and receiver tube was also experimented with in order to extract maximum performance out of the system. A comparison study was carried out to clearly know the intricacies of the different system and their arrangements and choose them meticulously according to our demands.

2.2. Research Gap

The potential of solar energy in India is immense. With our increasing population, our energy demands are also increasing. We look at solar power to help at fulfilling our energy needs throughout the year. Little research is documented that considers the operation of a PTC system on a monthly basis based on Indian conditions and also simultaneously account for the variation in input parameters. This study assesses the performance of a PTC system based on the conditions of New Delhi and also considers the variation in input parameters. The flow rate of fluid is also varied in order to know its effects on the performance of the system.

2.3. Objectives

The objective with which this work has been carried out is described in this section. The modeling of PTC is done by keeping in mind the following objectives:

- To assess the performance of a PTC for varying input variables. The variation in inputs is something that a concentrating collector will be subjected to throughout its working life. So it is vital that the variation in its performance be studied for these variations.

- To examine the year round performance of the collector. Other than hourly variation, the monthly variation in performance is also recorded to know the behavior of the system throughout the year.

- To examine the influence of variation in mass flow rate on the output of the system. The heat transfer fluid is passed with different flow rates to check how the system responds to these changes.

CHAPTER 3

SYSTEM DESCRIPTION

The overall arrangement of PTC with all its subsystems is described in this section. The development of this mathematical model is based upon the setup of PTC described here. The concentrator or reflector of the PTC has to focus the solar insolation over the receiver or absorber tube. To obtain higher heat gain, it is essential that the incidence angle of incoming radiation be minimum. This feat is achieved by making use of a Sun tracking mechanism. The collector is rotated about a single axis such that it follows the Sun throughout the day. The absorber tube is established at the focal axis of the concentrator and its setup direction is East West. The arrangement of concentrator along with the absorber tube is as presented in fig. 3.1. The absorber tube is a hollow tube with inside diameter D_i and outside diameter D_o. With an aim to increase the heat gain of heat transfer fluid, a twisted tape characterizing a twist ratio of 4 is also equipped inside the absorber tube. A glass cover outside the absorber tube acts as insulation. Outer diameter of glass cover is D_{co} and inside diameter is D_{ci}, whereas the aperture of concentrator is W. Air occupies the space between inside of cover and outside of absorber tube. The rate of heat gained by the heat transfer fluid depends upon the absorbed flux, which in turn depends upon the values of reflectivity of surface of the concentrator, transmissivity of the glass cover for solar irradiation, absorptivity of the absorber tube and intercept factor which is the ratio of the radiation seized by the receiver to the total radiation reflected by the concentrator. As the values of these parameters increase, the observed flux and therefore the rate of heat gain increases. The values of these radiation properties vary with the wavelength of incident thermal radiation, surface roughness of the body and also with its temperature. However, for the purpose of this mathematical model all these radiation properties are assumed as constant. The thermic fluid absorbs the heat energy due to the focusing of solar radiation over the absorber tube. This modeling procedure at all times, considers steady state heat transfer. This mathematical model calculates all the parameters of this system

ranging from efficiency, heat gain rate and fluid exit temperature. The parameters of the setup that are used as input variables are stated in Table 3.1.

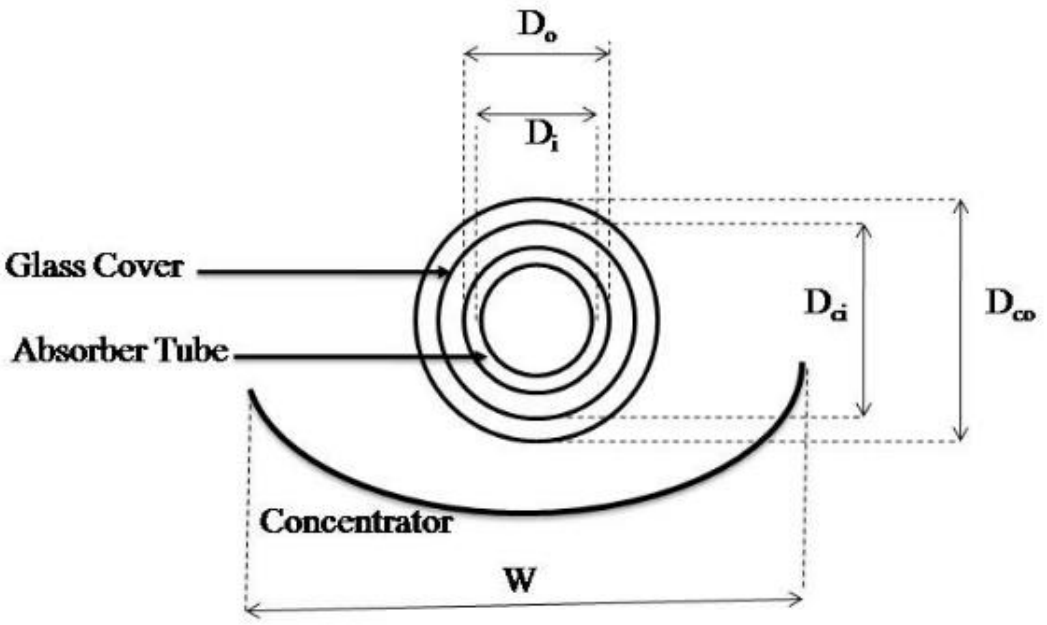

Fig. 3.1. Cross section of solar PTC with nomenclature [12]

Table 3.1: Characteristics of the system [12]

Parameters	**Value**
Location (New Delhi)	28°35’ N, 77°12’ E
Aperture of concentrator (W)	1.25 m
Length of concentrator (L)	3.657 m
Inner diameter of absorber tube (D_i)	0.0381 m
Outer diameter of absorber tube (D_o)	0.04135 m
Inner diameter of glass cover (D_{ci})	0.0560 m
Outer diameter of glass cover (D_{co})	0.0630 m
Tape twist ratio (x)	4
Reflectivity of concentrator (ρ)	0.85
Transmissivity of glass cover (τ)	0.85
Intercept factor (γ)	0.95
Emissivity/absorptivity of glass cover (ε_c)	0.88
Emissivity/absorptivity of absorber tube (ε_p)	0.95
Fluid inlet temperature (T_{fi})	50°C/323.15 K
Concentration ratio (C)	9.304
Ambient pressure (P_{atm})	101.325 KPa

CHAPTER 4

MATHEMATICAL MODELING

The modeling of the aforementioned setup is described here. The mathematical model associated with steady state is programmed based on Engineering Equation Solver (EES) numerical software. The performance analysis carried out in this work, comprising concepts and equations, is derived from [12].

The modeling of this work is based on certain assumptions that are detailed below.

- The complete system is assumed to be at steady state condition.
- Also, the pressure throughout the system is assumed atmospheric and deviation in pressure, if any, are neglected.
- The properties of the system together with that of thermic fluid are assumed constant and don not change over time, temperature or wavelength.
- Further, shading effect and dust accumulation are assumed to have no control on the working of the model.

The flux (S) that is absorbed in the absorber tube is expressed as:

$$S = I_b\, r_b\, \rho\gamma\, (\tau\alpha)_b + I_b\, r_b\, (\tau\alpha)_b \left(\frac{D_o}{W - D_o}\right) \tag{4.1}$$

where, I_b denotes the intensity of hourly beam radiation, r_b denoted the tilt factor for beam radiation, ρ denoted reflectivity of concentrator surface, intercept factor is γ, $(\tau\alpha)_b$ for beam radiation denotes transmissivity - absorptivity product, W denoted concentrator aperture, outside diameter of absorber is D_o.

The rate of useful heat gain is denoted by Q_u and expressed as:

$$Q_u = \left[S - \frac{U_l}{C} (T_{fi} - T_a) \right] F_r (W - D_o) L \tag{4.2}$$

It may also be written as:

$$Q_u = \dot{m} C_p (T_{fo} - T_{fi}) \quad (4.3)$$

Here, F_r denotes heat removal factor, U_l denotes overall loss coefficient, L denotes concentrator length, C denotes concentration ratio, T denotes temperature, subscript f denotes heat transfer fluid, subscript o denotes exit, subscript i denotes inlet and subscript a denotes ambient. F_r is expressed as a ratio of heat gain actual to heat gain possible if temperature throughout the absorber is T_{fi}, and it is written as:

$$F_r = \frac{\dot{m} C_p}{\pi D_o L U_l} \left[1 - \exp\left\{ - \frac{F' \pi D_o U_l L}{\dot{m} C_p} \right\} \right] \quad (4.4)$$

where, $\dot{m}$ is the mass flow rate of heat transfer fluid (HTF) in absorber tube, C_p is specific heat of HTF and F' is collector efficiency factor which is quiet similar to F_r, the only difference being the absorber tube temperature throughout is T_f instead of T_{fi}, defined as:

$$F' = \frac{1}{U_l \left(\frac{1}{U_l} + \frac{D_o}{D_i h_f} \right)} \quad (4.5)$$

where, D_i is the inside diameter of absorber tube and h_f is the convective heat transfer coefficient inside the absorber tube.

$$h_f = \frac{Nu_f * K_f}{D_i} \quad (4.6)$$

Here, f subscript denotes the fluid inside the absorber tube. The Nusselt number for absorber tube fluid is:

$$Nu_f = 5.172 \left[1 + 0.005484 \left\{ Pr \left(Re_f / x \right)^{1.78} \right\}^{0.7} \right]^{0.5} \quad (4.7)$$

where, x is the tape twist ratio in the absorber tube, Re_f is the Reynold number and Pr is the Prandtl number in the absorber.

C is expressed as a ratio of aperture area effective to absorber tube area, expressed as:

$$C = \frac{(W - D_o)}{\pi D_o} \quad (4.8)$$

U_l is vital in expressing the heat loss rate, which is written as:

$$Q_l = U_l \pi D_o L (T_{pm} - T_a) \quad (4.9)$$

The rate of heat loss can also be stated in terms of convection and radiation losses from the absorber tube and similarly, from the outside surface of the cover. From the assumption of steady state heat transfer, both these heat loss rate will be equal. Therefore, the rate of heat loss per unit length of the absorber tube is given as:

$$\frac{Q_l}{L} = h_{p\text{-}c} (T_{pm} - T_c) \pi Do + \frac{\sigma \pi D_o (T_{pm}^4 - T_c^4)}{\{\frac{1}{\varepsilon_p} + \frac{D_o}{D_{ci}} \left(\frac{1}{\varepsilon_c} - 1\right)\}} \quad (4.10)$$

$$\text{and, } \frac{Q_l}{L} = h_w (T_c - T_a) \pi D_{co} + \sigma \pi D_{co} \varepsilon_c (T_c^4 - T_{sky}^4) \quad (4.11)$$

Here, $h_{p\text{-}c}$ is the heat transfer coefficient for convection between absorber tube and cover due to the presence of motionless air molecules in the spacing between absorber tube and cover, h_w is the heat transfer coefficient for the outside of cover, "co" denotes the properties at the cover outer surface, "ci" denotes the cover inner surface, ε_p and ε_c is the emissivity of absorber and cover surface respectively.

An iterative methodology is followed to get the values of mean absorber tube temperature (T_{pm}) and cover temperature (T_c) from the above two equations. T_a denotes the ambient temperature and T_{sky} is the temperature of sky, taken as

$$T_{sky} = T_a - 6 \quad (4.12)$$

The collector instantaneous efficiency defined for only beam radiation is expressed as:

$$\eta_i = \frac{Q_u}{I_b r_b W L} \quad (4.13)$$

The optical efficiency of a collector is described as the ratio of solar insolation absorbed at the absorber to the total radiation received on the aperture, and it is written as:

$$\eta_o = \frac{S}{I_b r_b} \left(\frac{W - D_o}{W}\right) \quad (4.14)$$

CHAPTER 5

RESULTS AND DISCUSSION

The assessment of the current mathematical model is done by considering some variables with significant variations throughout the operation of PTC. Also, [9,12,19] are used for the validation of this model. The deviation in performance is similar to those presented in [12] and also in other research findings of [3, 9]. The validation of this model against [12] is expressed in Table 5.1.

Table 5.1. Validation of current model with the results in [12]

Parameters	**Model**	**Ref [12]**	**Variation**
Useful Heat Gain Rate	1299 Watts	1289.8 Watts	0.713%
Mean Absorber Temperature	441.3 K	441.13 K	0.0385%
Cover Temperature	334 K	333.39 K	0.1829%
Overall loss coefficient	13.13 W/m^2-K	13.27 W/m^2-K	1.055%
Exit fluid temperature	428.5 K	428.4 K	0.0233%
Instantaneous efficiency	39.73 %	39.5 %	0.582%

Table 5.2 presents the values of input parameters that are used for the validation of the model with [9] and Table 5.3 presents the validation against [9].

Table 5.2. Input parameters used for validation of model with [9]

Parameters	**Value**
Location (Bhiwani)	28°78’ N, 76°13’ E
Aperture area	38.45 m^2
Length of concentrator	7.8 m
Mass flow rate of thermal fluid	0.010 kg/s
Thermal fluid	Water
Fluid inlet temperature (T_{fi})	20°C/293 K
Fluid Exit temperature (T_{fo})	30.95°C/304.1 K
Angle of inclination	0
Concentration ratio (C)	22.42
Ambient pressure (P_{atm})	101.325 KPa

Table 5.3. Validation of the model against results in [9]

Parameters	**Model**	**Ref [9]**	**Variation**
Useful Heat Gain Rate	492.2 W	466.2 W	5.57%
Exit fluid temperature	304.8 K	304.1 K	0.23%
Instantaneous efficiency	63.6%	61.74%	3.012%

Table 5.4 presents the values of input parameters that are used for the validation of the model with [19] and Table 5.5 presents the validation against [19].

Table 5.4. Input parameters used for validation of model with [19]

Parameters	**Value**
Location (Gwalpahari)	28°25' N, 77°09' E
Aperture area	8175 m^2
Length of row	240 m
Loops	3 with U-type arrangement
Mass flow rate of thermal fluid	8.53 kg/s
Thermal fluid	Therminol VP-1
DNI	600 W/m^2
Capacity	3 MW
Fluid inlet temperature (T_{fi})	232°C/505.15 K
Fluid Exit temperature (T_{fo})	393°C/666.15 K
Inlet pressure	17.5 bar
Outlet pressure	13 bar

Table 5.5. Validation of the model against results in [19]

Parameters	Model	Ref [19]	Variation
Useful Heat Gain Rate	2.638 MW	3 MW	12.06%
Exit fluid temperature	370.45°C	393°C	5.74%
Instantaneous efficiency	49.28%	61.2%	19.47%

The intensity of beam radiation has substantial control over the performance of the system. This variation is attributed to the variation in the month of the year and also, the time of the day. Moreover, the value of environment temperature and velocity of wind changes with the month of the year and affects the performance. Further, the variation in the mass flow rate of the heat transfer fluid is used as a parameter to assess the changes in the performance parameters.

5.1. Results of year-round performance examination

In order to examine the year-round operating performance of the system, the key input variables were identified and the monthly variation in their values was considered for this analysis. Also, for year round performance, the mass flow rate of heat transfer fluid is assumed constant as 0.0986 kg/s. The monthly average change in solar beam radiation, ambient temperature and wind velocity data was collected and used for this analysis. Fig. 5.1 shows the variation of beam radiation against time of day. It was observed from the data in fig. 5.1 that the months of March to June receive significant solar insolation ranging from 624 W/m^2 being the highest of April and 115 W/m^2, of June, being the lowest of these four months with regard to the time of day considered [12].

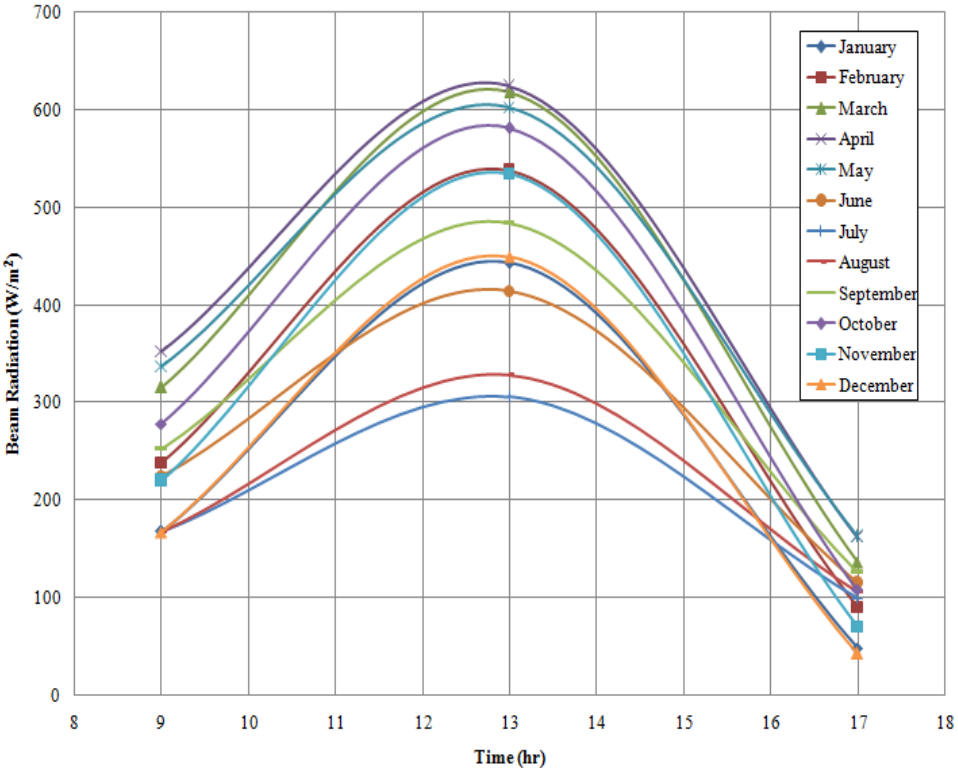

Fig. 5.1: Year round variation in beam radiation with time [12]

Owing to the high rate of heat gain, the thermal efficiency of collector increases when the beam radiation values increase with time. It is also attributed to the change in the solar incidence angle. Fig. 5.2 shows the variation of thermal efficiency with time of day and it can be inferred that the peak thermal efficiency is achieved at noon when the solar insolation is maximum and then it tends to decrease. The maximum thermal efficiency achieved varies with the month of the year with respect to time. Month of May produces maximum efficiency of the year at 59.57% followed by October and April at 59.12% and 58.93% respectively. The month of January attributes the lowest efficiency of the collector throughout the year at 46.13%, which is lower than 46.53% of August and 47.29% of July. The tilt factor, beam radiation and surrounding conditions influence the working of the system.

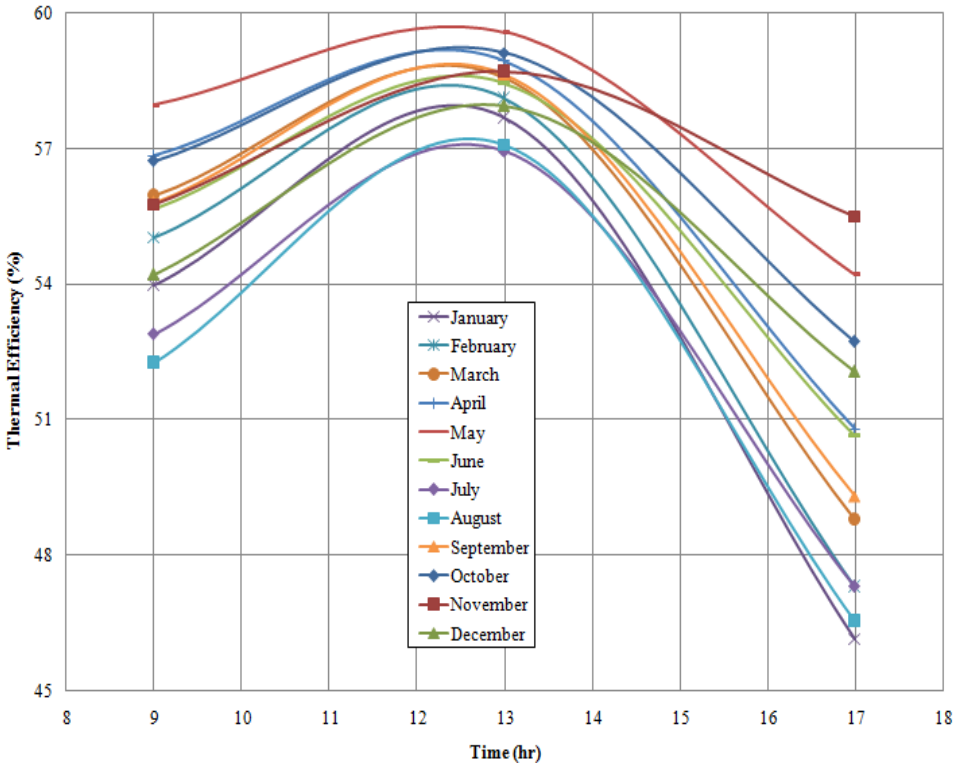

Fig. 5.2: Year round variation in thermal efficiency with time

Fig. 5.3 shows the variation of useful heat gain rate against time of day and gives the variation of useful heat gain rate with time for every month of an year. It presents that the highest value of useful heat is obtained for the month of November at 2151 W, followed by October at 2005 W and December with 1944 W. The maximum values are obtained at noon when the solar insolation is highest. It also shows that the values decrease as the intensity of beam radiation reduces later in the day, producing minimum 225.4 W in July and 226.5 W in August. This change in the value of useful heat gain is because of the high values of the overall loss coefficient for the months of March, April and May. It is also due to the lower values of heat removal factor for these months. Fig. 5.4 shows the variation of overall loss coefficient against time of day. It also shows that the month of May corresponds to the highest value of the overall loss coefficient i.e. 9.201 W/m^2-K, followed by March and April at 9.196 W/m^2-K and 9.181 W/m^2-K respectively. Similarly, fig. 5.5 shows the variation of collector heat removal factor against time of day and it also shows the lowest value of heat removal factor for March and May is 0.9426 each. These changes in heat

gain, loss coefficient and heat removal factor are owed to the intensity of beam radiation, the tilt factor and surrounding conditions of the collector.

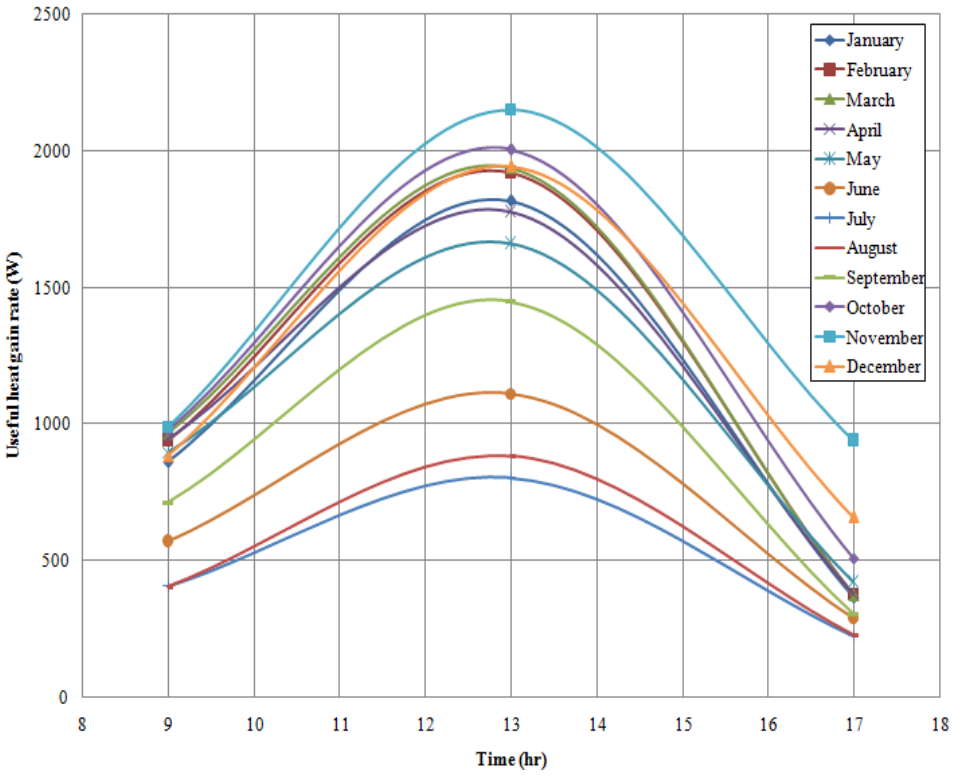

Fig. 5.3: Year round variation in rate of useful heat gain with time

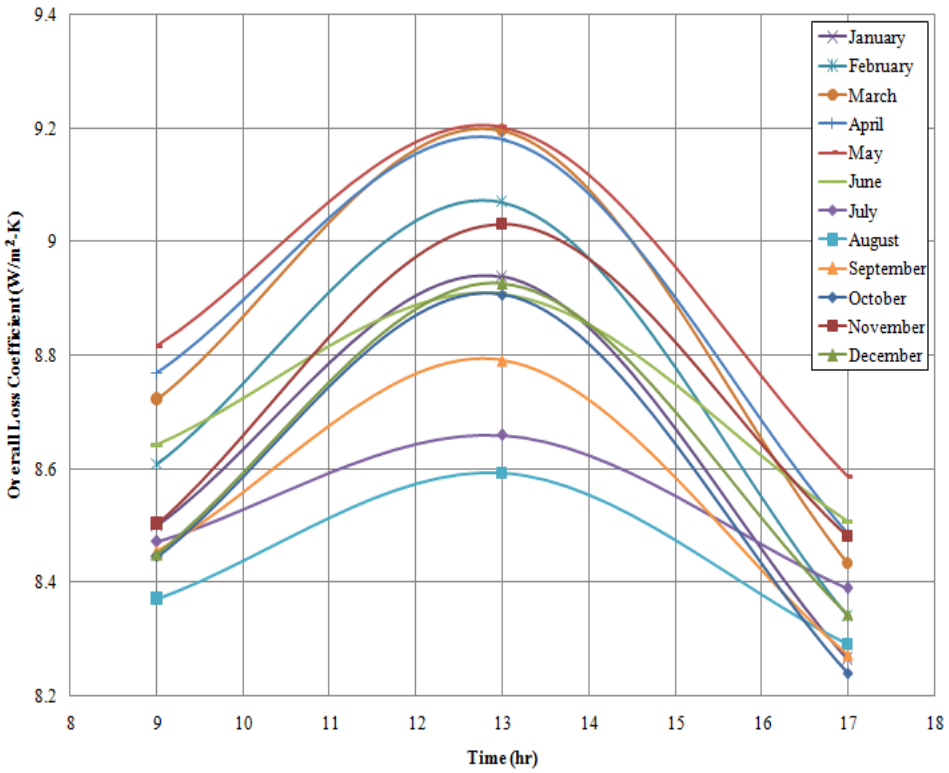

Fig. 5.4: Year round variation in overall loss coefficient with time

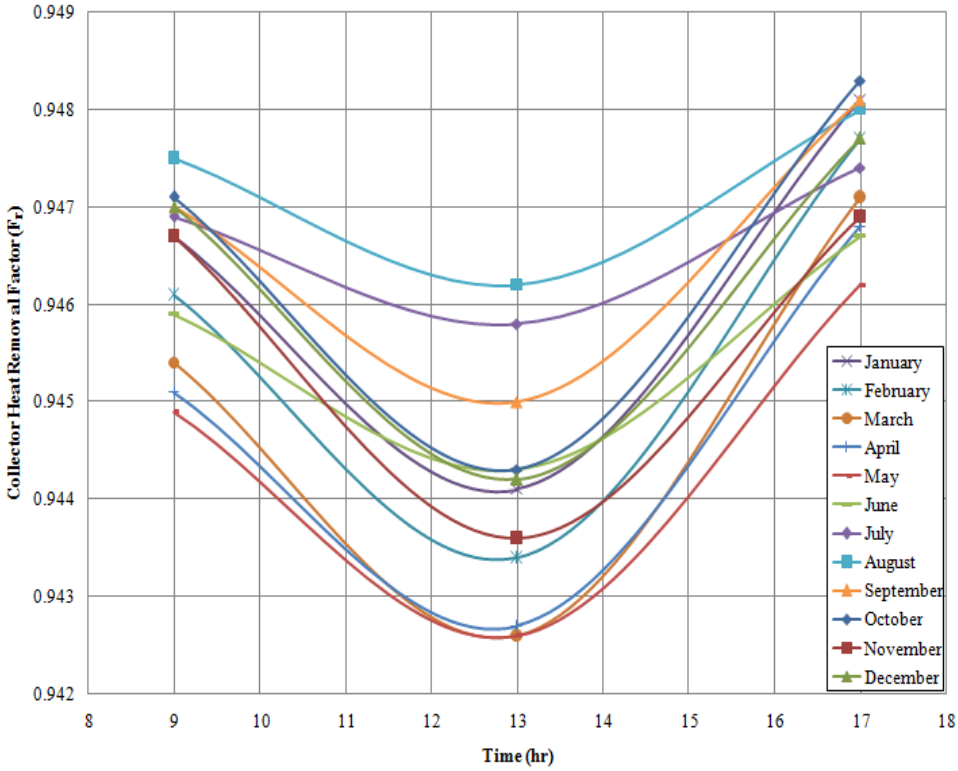

Fig. 5.5: Year round variation in heat removal factor with time

The aforementioned values of useful heat gain rate have significant effect on exit temperature of thermic fluid. Therefore, the variation of fluid exit temperature is similar to that of heat gain rate. Fig. 5.6 shows the variation of fluid exit temperature against time of day. As can be seen from fig. 5.6, the maximum value of exit temperature is obtained for the month of November at 332.1 K denoting a temperature increase of 8.95°C from the inlet fluid temperature whereas the lowest temperature of exit fluid is 324.1 K, a mere 0.95°C increase in temperature from inlet temperature, obtained for the months of July and August each. This variation is directly hinged with the heat gain variation as heat gain is the key parameter that influences the fluid exit temperature. The fluid temperature tends to increase as the day progresses and starts declining as the day approaches evening. At time of maximum solar insolation, a temperature difference of 5.6°C separates the highest temperature of fluid in November and the lowest temperature in July.

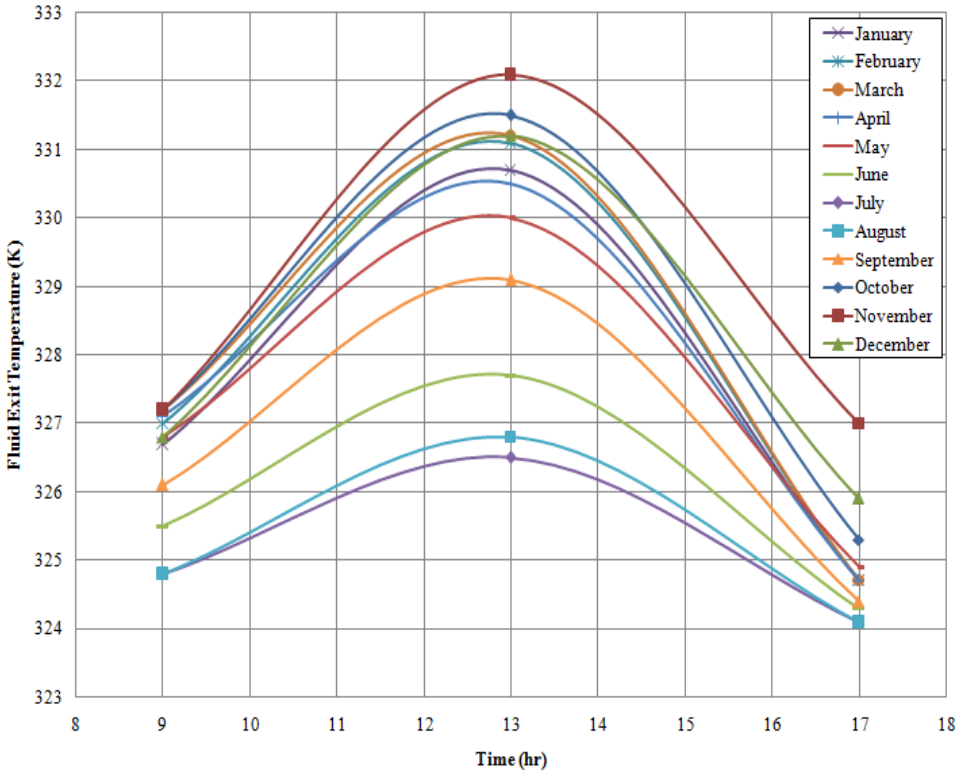

Fig. 5.6: Year round variation in fluid exit temperature with time

5.2. Results of fluid flow rate variations

In an attempt to assess the reaction of the system to the variations in input variables, the mass flow rate of the heat transfer fluid is varied. Three independent mass flow rate values are used and the parameters of the system are examined correspondingly. The values used for this model are 0.0986 kg/s, 0.0886 kg/s and 0.0786 kg/s. The effects of flow rate variations were calculated using this mathematical model and they showed relevance and agreement with the behavior stated in [12]. The performance investigation is done for various times of the day for the month of May and the variations are presented in the form of curves.

Fig. 5.7 shows the variation of useful heat gain rate with time of day for variable flow rate. It may be inferred from this curve that the heat gain is maximum when the flow rate is increased. Although, the increase is not very substantial, it is vital for the increase in overall performance. The maximum value of heat gain is obtained at noon with a value of 1662 W, 1654 W and 1644 W for flow rates of 0.0986 kg/s, 0.0886 kg/s and 0.0786 kg/s respectively. The difference between respective maximum and

minimum values at noon is of 18 W which is a mere 1.083 % of the maximum value. The minimum value for the day is obtained in the morning from where it increases till noon and again decreases from here till evening. This variation is attributed to the beam radiation values of the day. Also, fig. 5.8 shows the variation of overall loss coefficient against time of day for variable flow rate and it also shows that when the flow rate of thermic fluid is increased, the values of overall loss coefficient are decreased. This decrease in the value of loss coefficient adds to the increase in heat gain. Fig. 5.9 shows the variation of collector heat removal factor with time of day for variable flow rate. Moreover, the heat removal factor increases with the increase in flow rate as shown in fig. 5.9, further increasing the heat gain. However, this increase is not very surplus and the addition in heat gain with increase in flow rate is only marginal. The minimum obtained value of heat gain is 150.8 W for 0.0786 kg/s and increases with the flow rate to 151.5 W for 0.0886 kg/s and 152.2 W for 0.0986 kg/s. The difference between respective maximum and minimum values of heat gain in the morning is just 1.4 W, 0.91 % of the maximum, which is less than that for noon. A similar value of 1.4 W is obtained for evening too. Therefore, it is inferred that the increase in useful heat gain with the flow rate at a specific time of the day is higher in the noon compared to the increase in mornings and evenings.

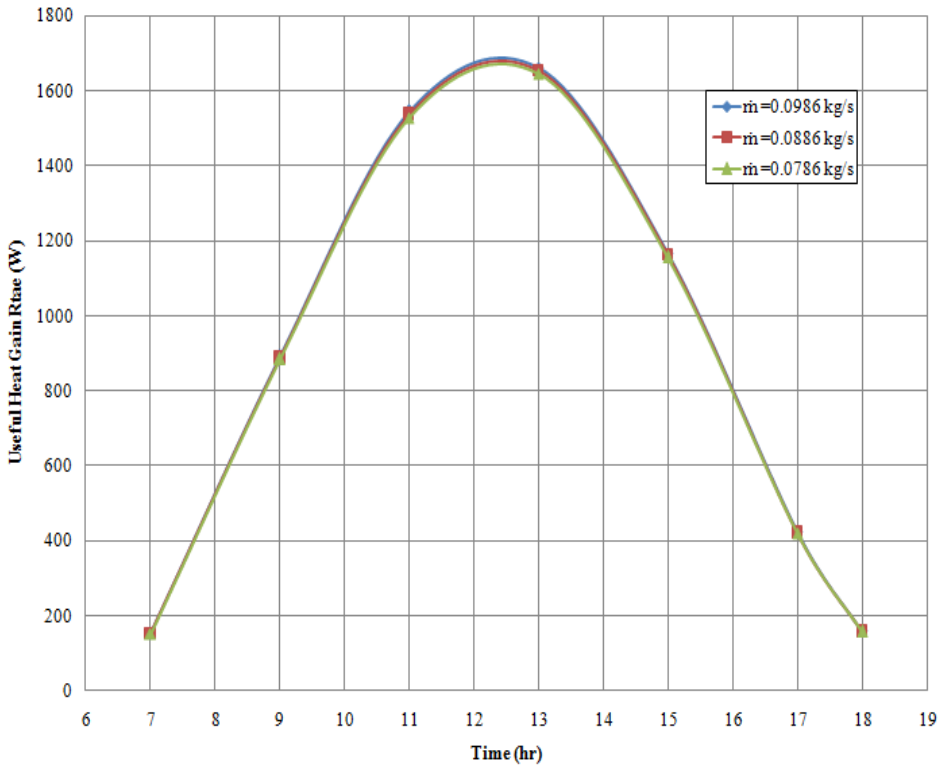

Fig. 5.7: Variation in useful heat gain with time for different flow rates

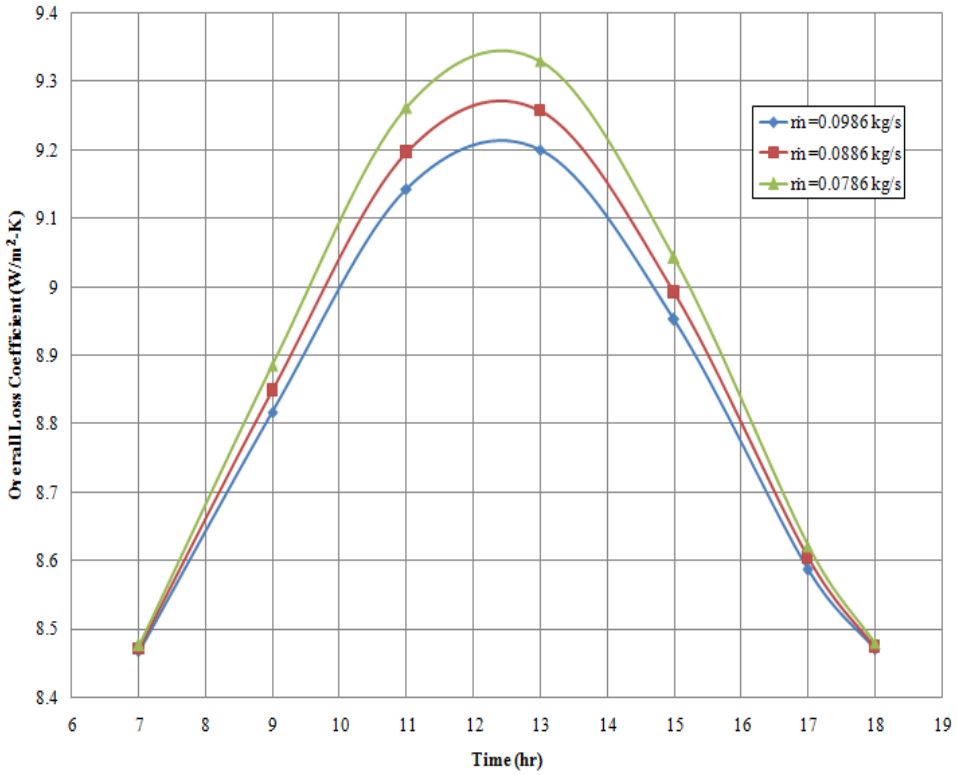

Fig. 5.8: Variation in overall loss coefficient with time for different flow rates

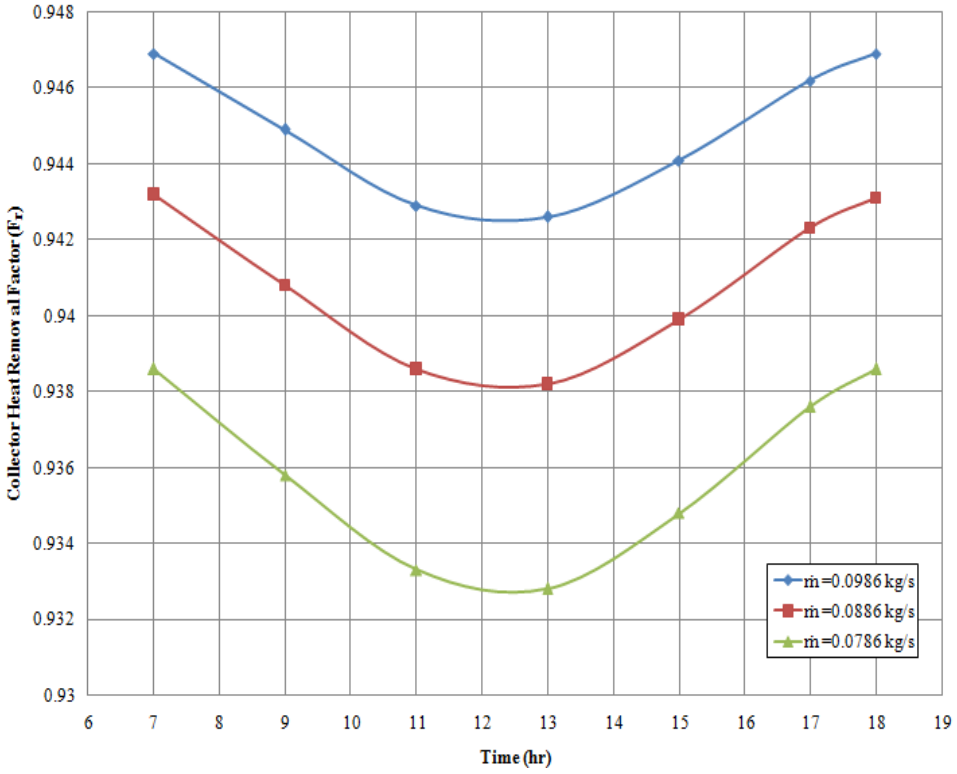

Fig. 5.9: Variation in heat removal factor with time for different flow rates

Fig. 5.10 shows the variation of thermal efficiency with time of day for variable flow rate. The efficiency is directly related to the heat gain rate and hence, the trend of efficiency is similar to that of heat gain. The maximum efficiency obtained in the system is 59.57 % at noon for the maximum mass flow rate i.e. 0.0986 kg/s. It is followed by 59.28 % and 58.92 % for flow rates 0.0886 kg/s and 0.0786 kg/s respectively. The difference between maximum efficiency and minimum efficiency at noon is 0.65 %. This value is 0.41 % for morning and evening each. So, it may be emphasized that the increase in thermal efficiency with flow rate at a particular time of the day is maximum at noon compared with the morning and evening.

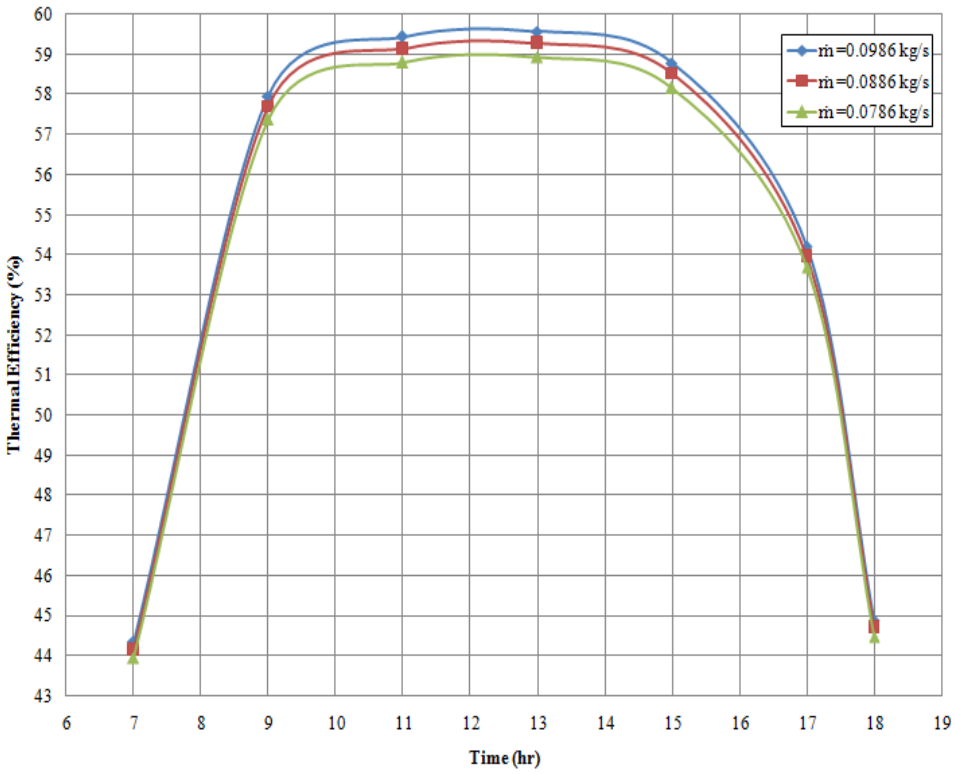

Fig. 5.10: Variation in thermal efficiency with time for different flow rates

Exit temperature of fluid is another vital performance parameter that has to be examined. Fig. 5.11 shows the variation of fluid exit temperature with time of day for variable flow rate and it also shows the variation trend of temperature at exit with regard to the time of day for different flow rates of heat transfer fluid. It is presented that the exit temperature is decreased as the flow rate of thermic fluid is increased. The maximum temperature obtained is 331.7 K at a flow rate of 0.0786 kg/s and this value of temperature is decreased to 330.8 K and 330 K for flow rates of 0.0886 kg/s and 0.0986 kg/s respectively. The maximum temperature values are obtained at noon

which is reduced in the mornings and evenings. The increase in maximum temperature with decrease in flow rate is 1.7°C at noon. This increase is 0.1°C in morning and 0.2°C in the evening. In spite of the heat gain increasing with the flow rate, the fluid temperature at exit decreases because of the increase in mass flow rate. It is derived from fig. 5.7 that the increase in maximum heat gain by increasing the flow rate is 1.095 % but the increase in flow rate of thermic fluid is 25.44 %. This much higher escalation in the flow rate concludes in decreasing the exit temperature of fluid. Therefore, it is stated that the raise in the temperature is more substantial in the noon compared with that in the morning and evening.

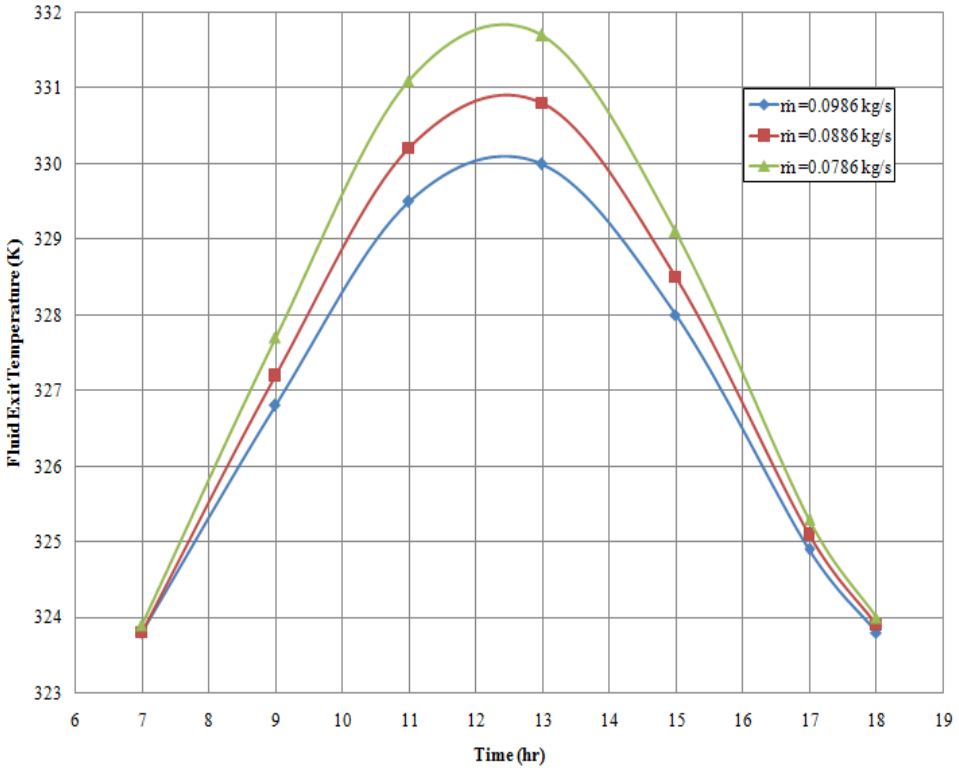

Fig. 5.11: Variation in exit temperature of fluid with time for different flow rates

CHAPTER 6

CONCLUSIONS AND FUTURE SCOPE

6.1. Conclusions

A steady state mathematical model is developed in this work that presents extensive examination of the operating parameters of a solar parabolic trough collector. The model is validated by results in previous studies. The year round performance of the PTC is obtained using this model and also, the heat transfer fluid's mass flow rate is changed to check the performance response of the system for variations in input variables. The following conclusions can be made:

- Year round examination of parameters yields the maximum thermal efficiency of 59.57 % for the month of May, followed by 59.12 % for October and 58.93 % for April. The lowest efficiency is for the month of January at 46.13 %.

- The maximum value of rate of heat gain is 2151 W for the month of November, followed by 2005 W for October and 1944 W for December. The lowest obtained value is 225.4 W for the month of July.

- The maximum difference in fluid exit and inlet temperature is obtained for the month of November which is 8.95°C. The minimum value of this temperature difference is 0.95°C, obtained for both July and August. At noon, the difference between maximum fluid exit temperature for November and July is 5.6°C.

- On varying the flow rate of thermic fluid, it was found that the rate of heat gain is increasing with increased flow rate. A maximum value of 1662 W is obtained for maximum flow rate of 0.0986 kg/s and lowest value of 1644 W for flow rate 0.0786 kg/s is obtained. At noon, the difference between maximum heat gain for varying flow rate is 18 W, 1.083 % of maximum

value. The increase in heat gain by escalating the flow rate is higher at noon than the morning or evening.

- The maximum thermal efficiency of 59.57 % is obtained for the maximum flow rate of 0.0986 kg/s and the minimum value is 58.92 % for lowest flow rate of 0.0786 kg/s. At noon, the raise in thermal efficiency with the flow rate is 0.65 %. This increase with increasing flow rate is higher at noon than in the morning or evening.

- Temperature of exit fluid is maximum for the minimum flow rate and it tends to decrease as the flow rate rises. Maximum temperature obtained is 331.7 K for flow rate of 0.0786 kg/s and the lowest temperature is 330 K for flow rate 0.0986 kg/s. At noon, the increase in maximum temperature with decrease in flow rate is 1.7°C. This increase in temperature is more significant in the noon compared with that in the morning and evening.

6.2. Future Scope

There is immense scope for future assessment that can be done in this field. Some of them are stated below:

- The feasibility study of this system can be carried out with emphasis on economic factors.

- The suitability of the system can be checked with respect to different locations.

References

[1] Ministry of New and Renewable Energy (MNRE), Government of India. Annual Report 2019-20. Accessed on: June 25, 2020. [Online]. Available: https://mnre.gov.in/img/documents/uploads/file_f-1585710569965.pdf

[2] Kalogirou SA. Solar Energy Engineering: Processes and systems. 2nd Edition. Elsevier Inc. 2014. https://doi.org/10.1016/C2011-0-07038-2

[3] Huang W, Hu P, Chen Z (2012). Performance simulation of a parabolic trough solar collector. Solar Energy; Vol. 86 No. 2: pp. 746-755. https://doi.org/10.1016/j.solener.2011.11.018

[4] Siva Subramanian R, Kumaresan G, Palanivel R, Nishanth Kalathil P, Nirmal B (2020). Comparative performance analysis of parabolic trough solar collector by varying absorber surface. Materials Today: Proceedings. [in press]. https://doi.org/10.1016/j.matpr.2020.04.248

[5] Quezada-Garcia S, Sanchez-Mora H, Polo-Labarrios MA, Cazares-Ramirez RI (2019). Modelling and simulation to determine the thermal efficiency of a parabolic solar trough collector system. Case Studies in Thermal Engineering; Vol. 16: 100523. https://doi.org/10.1016/j.csite.2019.100523

[6] Arun CA, Sreekumar PC (2018). Modelling and performance evaluation of parabolic trough solar collector desalination system. Materials Today:Proceedings; Vol. 5 No. 1: pp. 780-788. https://doi.org/10.1016/j.matpr.2017.11.147

[7] Conrado LS, Rodriguez-Pulido A, Calderon G (2017). Thermal performance of parabolic trough solar collectors. Renewable and sustainable energy reviews; Vol. 67: pp. 1345-1359. https://doi.org/10.1016/j.rser.2016.09.071

[8] Qu W, Wang R, Hong H, Sun J, Jin H (2017). Test of a solar parabolic trough collector with rotatable axis tracking. Applied Energy; Vol. 207: pp. 7-17. https://doi.org/10.1016/j.apenergy.2017.05.114

[9] Kumar D, Kumar S (2015). Year-round performance assessment of a solar parabolic trough collector under climatic condition of Bhiwani, India: A case study. Energy Conversion and Management; Vol. 106: pp. 224-234. https://doi.org/10.1016/j.enconman.2015.09.044

[10] Lozano-Medina A, Manzano L, Marcos JD and Blanco-Marigorta AM. (2019). Design of a concentrating solar thermal collector installation for a hotel complex in Gran Canaria. Energy; Vol. 183: pp. 803–811. https://doi.org/10.1016/j.energy.2019.06.165

[11] Zou B, Dong J, Yao Y and Jiang Y. (2016). An experimental investigation on a small-sized parabolic trough solar collector for water heating in cold areas. Applied Energy; Vol. 163: pp. 396–407. https://doi.org/10.1016/j.apenergy.2015.10.186

[12] Sukhatme JP and Nayak JK (2014). Solar Energy: Principles of thermal collection and storage; 3rd edition. McGraw Hill Education (New Delhi).

[13] Zou B, Jiang Y, Yao Y and Yang H. (2019). Impacts of non-ideal optical factors on the performance of parabolic trough solar collectors. Energy 2019; Vol. 183: pp. 1150-1165. https://doi.org/10.1016/j.energy.2019.07.024

[14] Aguilar R, Valenzuela L, Avila-Marin AL and Garcia-Ybarra PL. (2019). Simplified heat transfer model for parabolic trough solar collectors using supercritical CO_2. Energy Conversion and Management; Vol. 196: pp. 807–820. https://doi.org/10.1016/j.enconman.2019.06.029

[15] Khakrah H, Shamloo A and Kazemzadeh Hannani S. (2018). Exergy analysis of parabolic trough solar collectors using Al_2O_3/synthetic oil nanofluid. Solar Energy; Vol. 173: pp. 1236–1247. https://doi.org/10.1016/j.solener.2018.08.064

[16] Bellos E and Tzivanidis C. (2019). Alternative designs of parabolic trough solar collectors. Progress in Energy and Combustion Science; Vol. 71: pp. 81–117. https://doi.org/10.1016/j.pecs.2018.11.001

[17] Tyagi SK, Wang S, Singhal MK, Kaushik SC and Park SR. (2007). Exergy analysis and parametric study of concentrating type solar collectors. International

Journal of Thermal Sciences; Vol. 46 No. 12: pp. 1304-1310. https://doi.org/10.1016/j.ijthermalsci.2006.11.010

[18] Ghasemi SE, Ranjbar AA. (2016). Thermal performance analysis of solar parabolic trough collector using nanofluid as working fluid: A CFD modelling study. Journal of Molecular Liquids; Vol. 222: pp. 159-166. https://doi.org/10.1016/j.molliq.2016.06.091

[19] Nayak JK, Kedare SB, Banerjee R, Bandyopadhyay S, Desai NB, Paul S, Kapila A. A 1 MW national solar thermal research cum demonstration facility at Gwalpahari, Haryana, India. Current Science; Vol. 109 No. 8: pp. 1445-1457. 10.18520/v109/i8/1445-1457

APPENDIX 1

Monthly Data

Time / Month	09:00	13:00	17:00
January	168	443	48
February	238	538	90
March	316	618	136
April	352	624	162
May	337	602	163
June	224	414	115
July	168	306	99
August	168	328	106
September	253	484	126
October	278	581	108
November	220	534	70
December	167	449	43

Table A 1.1: Monthly Beam Radiation Data for New Delhi (28°35' N, 77°12' E)

Month	Ambient Temperature (K)	Wind Speed (m/s)	Average number of day (n)
January	288.706	2.905	15
February	291.483	3.13	46
March	295.928	3.44	74
April	300.928	3.53	105
May	307.039	3.62	135
June	305.928	3.59	166
July	304.261	3.17	196
August	302.594	2.77	227
September	301.483	2.59	258
October	298.15	2.28	288
November	293.15	2.59	319
December	288.706	2.68	349

Table A 1.2: Monthly average ambient temperature, wind speed for New Delhi (28°35' N, 77°12' E) and Number of day data

APPENDIX 2

Monthly Results

Time	ω	S	T_{pm}	T_c	F_r	U_L	Q_u	T_{fo}	η_i
09:00	-52.62	237.4	335.2	296.9	0.9467	8.499	861.8	326.7	53.97
13:00	7.378	468.6	348.5	300.2	0.9441	8.938	1817	330.7	57.67
17:00	67.38	117.8	328.2	295.3	0.9481	8.265	365.6	324.7	46.13

Table A 2.1: Monthly results for the month of January

Time	ω	S	T_{pm}	T_c	F_r	U_L	Q_u	T_{fo}	η_i
09:00	-53.94	254	336.2	299.1	0.9461	8.608	939.8	327	55.01
13:00	6.057	491.6	349.9	302.3	0.9434	9.07	1921	331.1	58.11
17:00	66.06	118	328.4	297.4	0.9477	8.341	375.5	324.7	47.3

Table A 2.2: Monthly results for the month of February

Time	ω	S	T_{pm}	T_c	F_r	U_L	Q_u	T_{fo}	η_i
09:00	-52.71	256.8	336.6	302.5	0.9454	8.723	966.3	327.2	55.96
13:00	7.286	492.2	350.2	305.5	0.9426	9.196	1939	331.2	58.56
17:00	67.29	114	328.4	300.8	0.9471	8.433	374.1	324.7	48.78

Table A 2.3: Monthly results for the month of March

Time	ω	S	T_{pm}	T_c	F_r	U_L	Q_u	T_{fo}	η_i
09:00	-50.36	246.6	336.3	306.4	0.9451	8.769	942.6	327.1	56.84
13:00	9.644	448.7	347.9	308.9	0.9427	9.181	1778	330.5	58.93
17:00	69.64	110.3	328.4	304.8	0.9468	8.488	376.6	324.7	50.78

Table A 2.4: Monthly results for the month of April

Time	ω	S	T_{pm}	T_c	F_r	U_L	Q_u	T_{fo}	η_i
09:00	-49.36	229.1	335.6	311.1	0.9449	8.817	893	326.8	57.96
13:00	10.64	414.8	346.3	313.4	0.9426	9.201	1662	330	59.57
17:00	70.64	116	329	309.8	0.9462	8.587	422.8	324.9	54.21

Table A 2.5: Monthly results for the month of May

Time	ω	S	T_{pm}	T_c	F_r	U_L	Q_u	T_{fo}	η_i
09:00	-50.36	152.9	331.1	309.4	0.9459	8.642	572.6	325.5	55.66
13:00	9.64	282.5	338.6	310.9	0.9443	8.908	1110	327.7	58.44
17:00	69.64	84.61	327.2	308.6	0.9467	8.508	288.1	324.3	50.64

Table A 2.6: Monthly results for the month of June

Time	ω	S	T_{pm}	T_c	F_r	U_L	Q_u	T_{fo}	η_i
09:00	-51.7	114.4	328.8	307.7	0.9469	8.472	407	324.8	52.88
13:00	8.296	209.5	334.3	308.9	0.9458	8.659	802.2	326.5	56.94
17:00	68.3	70.85	326.3	307.2	0.9474	8.39	225.4	324.1	47.29

Table A 2.7: Monthly results for the month of July

Time	ω	S	T_{pm}	T_c	F_r	U_L	Q_u	T_{fo}	η_i
09:00	-51.32	115.1	328.8	306.6	0.9475	8.371	404.5	324.8	52.26
13:00	8.676	230.4	335.5	308.1	0.9462	8.592	884.3	326.8	57.06
17:00	68.68	72.37	326.3	306.1	0.948	8.291	226.5	324.1	46.53

Table A 2.8: Monthly results for the month of August

Time	ω	S	T_{pm}	T_c	F_r	U_L	Q_u	T_{fo}	η_i
09:00	-48.88	190.1	333.1	306.8	0.947	8.455	713.2	326.1	55.79
13:00	11.12	367	343.3	309.2	0.945	8.791	1448	329.1	58.64
17:00	71.12	92.21	327.4	305.5	0.9481	8.272	305.7	324.4	49.29

Table A 2.9: Monthly results for the month of September

Time	ω	S	T_{pm}	T_c	F_r	U_L	Q_u	T_{fo}	η_i
09:00	-46.56	255.9	336.7	305.4	0.9471	8.446	976.1	327.2	56.72
13:00	13.44	504.2	351.1	309.1	0.9443	8.907	2005	331.5	59.12
17:00	73.44	143.7	330.2	303.8	0.9483	8.24	509.3	325.3	52.72

Table A 2.10: Monthly results for the month of October

Time	ω	S	T_{pm}	T_c	F_r	U_L	Q_u	T_{fo}	η_i
09:00	-46.61	263.3	336.9	301.2	0.9467	8.504	987.1	327.2	55.74
13:00	13.39	544.8	353.1	305.3	0.9436	9.031	2151	332.1	58.7
17:00	73.39	251.9	336.2	301	0.9469	8.481	939.6	327	55.47

Table A 2.11: Monthly results for the month of November

Time	ω	S	T_{pm}	T_c	F_r	U_L	Q_u	T_{fo}	η_i
09:00	-49.34	242.5	335.5	297.3	0.947	8.449	884.2	326.8	54.21
13:00	10.66	498.9	350.2	301	0.9442	8.926	1944	331.2	57.94
17:00	70.66	188.3	332.3	296.5	0.9477	8.344	659.3	325.9	52.06

Table A 2.12: Monthly results for the month of December

APPENDIX 3

Flow rate variation results

Time	ω	S	T_{pm}	T_c	F_r	U_L	Q_u	T_{fo}	n_i
07:00	-79.36	51.02	325.3	309.2	0.9469	8.468	152.2	323.8	44.35
09:00	-49.36	229.1	335.6	311.1	0.9449	8.817	893	326.8	57.96
11:00	-19.36	386.5	344.7	313	0.9429	9.143	1545	329.5	59.43
13:00	10.64	414.8	346.3	313.4	0.9426	9.201	1662	330	59.57
15:00	40.64	295.2	339.4	311.9	0.9441	8.953	1167	328	58.78
17:00	70.64	116	329	309.8	0.9462	8.587	422.8	324.9	54.21
18:00	85.64	52.65	325.4	309.2	0.9469	8.471	158.9	323.8	44.89

Table A 3.1: Results with flow rate of 0.0986 kg/s.

Time	ω	S	T_{pm}	T_c	F_r	U_L	Q_u	T_{fo}	η_i
07:00	-79.36	51.02	325.4	309.2	0.9432	8.471	151.5	323.8	44.16
09:00	-49.36	229.1	336.5	311.3	0.9408	8.849	888.9	327.2	57.69
11:00	-19.36	386.5	346.2	313.3	0.9386	9.197	1537	330.2	59.14
13:00	10.64	414.8	347.9	313.7	0.9382	9.258	1654	330.8	59.28
15:00	40.64	295.2	340.5	312.1	0.9399	8.992	1162	328.5	58.51
17:00	70.64	116	329.5	309.9	0.9423	8.604	420.9	325.1	53.97
18:00	85.64	52.65	325.5	309.2	0.9431	8.474	158.3	323.9	44.71

Table A 3.2: Results with flow rate of 0.0886 kg/s.

Time	ω	S	T_{pm}	T_c	F_r	U_L	Q_u	T_{fo}	η_i
07:00	-79.36	51.02	325.6	309.2	0.9386	8.477	150.8	323.9	43.94
09:00	-49.36	229.1	337.5	311.5	0.9358	8.885	884	327.7	57.37
11:00	-19.36	386.5	348	313.7	0.9333	9.262	1528	331.1	58.79
13:00	10.64	414.8	349.9	314.2	0.9328	9.33	1644	331.7	58.92
15:00	40.64	295.2	341.9	312.4	0.9348	9.043	1155	329.1	58.17
17:00	70.64	116	330	310	0.9376	8.621	418.7	325.3	53.69
18:00	85.64	52.65	325.7	309.2	0.9386	8.48	157.5	324	44.48

Table A 3.3: Results with flow rate of 0.0786 kg/s.